

Accuracy of laser tracker measurements of the GMT 8.4 m off-axis mirror segments

Tom L. Zobrist^{a,b}, James H. Burge^{a,b}, Hubert M. Martin^b

^aCollege of Optical Sciences, University of Arizona, Tucson, AZ 85721, USA

^bSteward Observatory, University of Arizona, Tucson, AZ 85721, USA

ABSTRACT

We have developed a metrology system that is capable of measuring rough ground and polished surfaces alike, has limited sensitivity to the nominal surface shape, and can accommodate surfaces up to 8.4 m in diameter. The system couples a commercial laser tracker with an advanced calibration technique and a system of stability references to mitigate numerous error sources. This system was built to guide loose abrasive grinding and initial polishing of the off-axis primary mirror segments for the Giant Magellan Telescope (GMT), and is also being used to guide the fabrication of the Large Synoptic Survey Telescope primary and tertiary mirrors. In addition to guiding fabrication, the system also works as a verification test for the GMT principal optical interferometric test of the polished mirror segment to corroborate the measurement in several low-order aberrations. A quantitative assessment of the system accuracy is presented, along with measurement results for GMT, including a comparison to the optical interferometric test of the polished surface.

telescopes, optical fabrication, optical testing, laser metrology, aspheres

1. INTRODUCTION

This paper details the system accuracy of an advanced metrology instrument designed to guide the fabrication of large telescope mirror segments during loose-abrasive grinding. The instrument, referred to as the Laser Tracker Plus system, couples a commercial laser tracker with an advanced calibration technique and a system of stability references to mitigate numerous error sources.^{1 2} The Laser Tracker Plus system also works as a verification test to corroborate the optical interferometric test of the polished mirror, in several low-order aberrations.

This system was designed specifically to guide the loose-abrasive grinding of the Giant Magellan Telescope (GMT) primary mirror segments.³ The GMT design uses seven 8.4 m mirror segments arranged in a close pack structure that produces an $f/0.7$ ellipsoidal parent mirror with an effective aperture of about 25 m.⁴ The central segment is on-axis, while the surrounding six segments are all off-axis. Each of the six identical off-axis segments has a best-fit radius of curvature (RoC) of 38 m, and 14.5 mm of peak to valley aspheric departure.⁵ Figure 1 shows a computer image depicting GMT. New methods and hardware were developed to test GMT because of the off-axis nature of the segment, the very large aspheric departure, and the long RoC.⁶

During loose-abrasive grinding and initial polishing of the GMT segment, the optical surface was periodically measured using the laser tracker mounted 22.3 m above the mirror surface in the test tower.⁷ To measure the segment, a sphere-mounted retroreflector (SMR), which is a retroreflecting corner-cube mounted in a small steel sphere with the corner of the cube at the center of the sphere, is moved across the surface and its position is measured by the laser tracker. A set of stability references is used to improve the accuracy of these measurements by compensating for rigid-body motion and refractive index variations. A minimum system accuracy of 2 μm rms over the entire surface of the segment was required in order to guarantee that interference fringes would be resolved when the transition from Laser Tracker Plus to interferometric testing was made. Furthermore, to provide

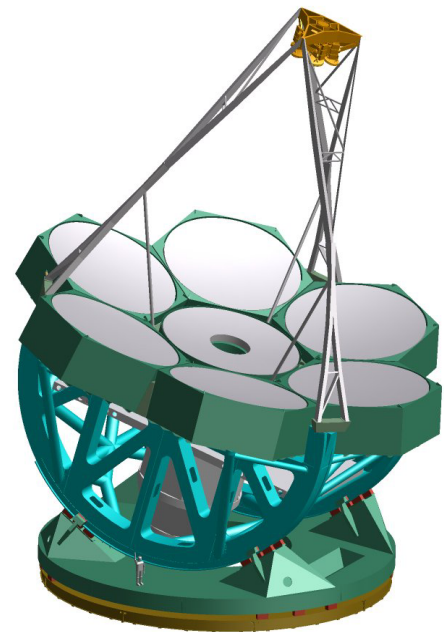


Figure 1: The 25 m $f/0.7$ GMT primary mirror is made of 8.4-m diameter segments.

corroboration of the optical interferometric test of the surface, the system must accurately measure low-order aberrations to about $0.5 \mu\text{m}$ rms surface.

To achieve these accuracies with a laser tracker when testing a large mirror, we have added:

- Stability references that compensate for rigid-body motion and large-scale variations in refractive index, discussed in Section 2, and
- An advanced calibration of the laser tracker to improve the angular accuracy, discussed in Section 4.

This enhanced system is the Laser Tracker Plus system, shown in Figure 2, which fulfills two important functions:

- It does not require a specular surface, so it can be used to measure the rough surface for guiding the generating and loose abrasive grinding operations.
- It can measure low order shape errors in the polished surface to $< 1 \mu\text{m}$, providing independent corroboration of these components of the mirror shape.

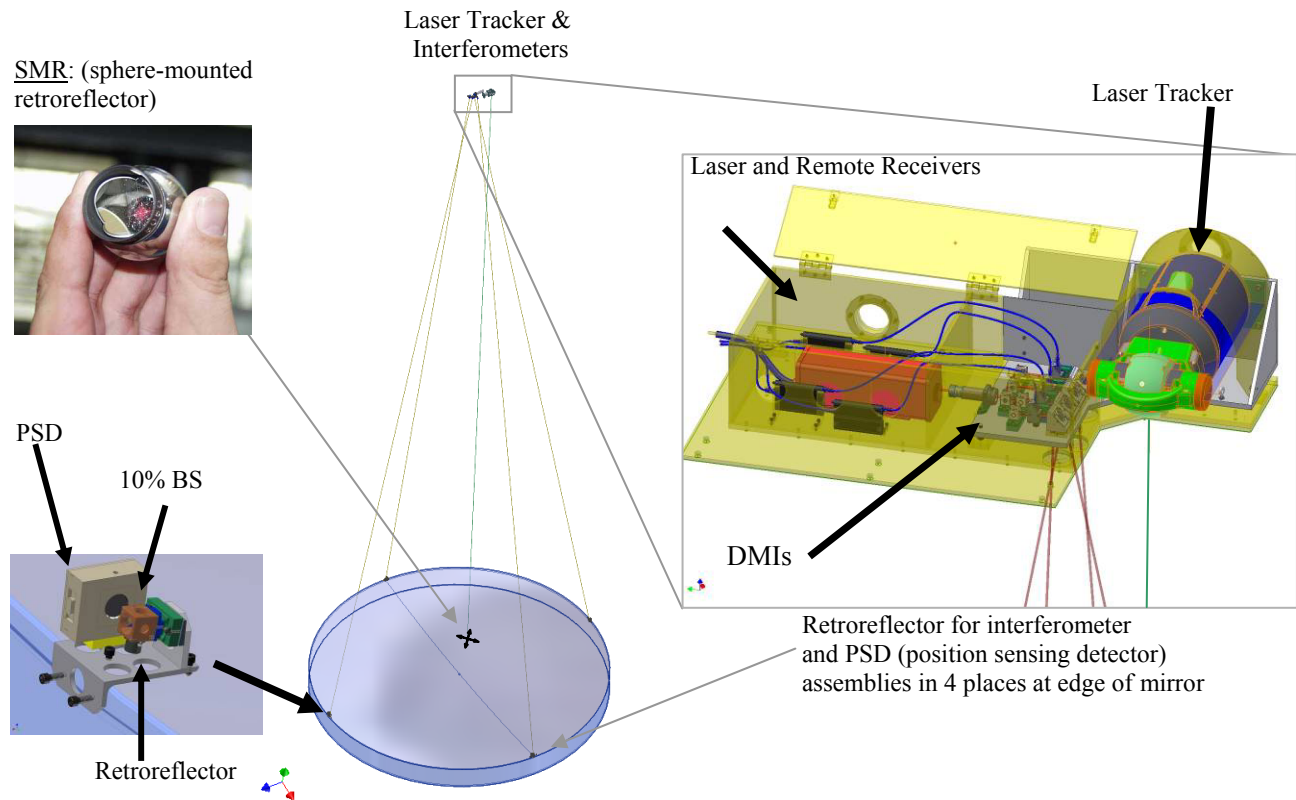


Figure 2: Conceptual drawing of the laser tracker set up for measuring the mirror surface. The laser tracker uses interferometry to measure distance to an SMR (sphere-mounted retroreflector). The tracker runs under servo control to follow the SMR as it is scanned across the surface, combining radial distance with the gimbal angles to make a three-dimensional measurement. Effects due to the combined motion of the air, mirror, and tracker are mitigated by separate real-time measurements of distance and lateral motion using a system of four stability references.

The design of the Laser Tracker Plus system was driven by a set of performance requirements and goals that are based on the manufacturing specifications for the GMT segments.⁸ The segment specifications include tight tolerances on radius of curvature, off-axis distance and clocking angle, each of which corresponds to a particular low-order aberration or combination of aberrations. For example, an error in off-axis distance is equivalent to a combination of power, astigmatism, and coma in the surface.³ The segment specification also allows limited amounts of low-order aberrations like astigmatism that can be corrected at the telescope with the active mirror support and realignment of the segment. Table 1 lists the top-level requirements and goals for each category, and some implied requirements.

Table 1: Requirements and goals for the Laser Tracker Plus system.

Top-level requirement	Implied requirements
Minimum requirements	
<ol style="list-style-type: none"> 1. Guide figuring to within capture range of principal optical test. 2. Reduce geometry errors (RoC, off-axis distance, clocking) to levels that can be corrected by polishing (~10 μm P-V surface). 	<ol style="list-style-type: none"> 1. Net accuracy of 2 μm rms for first 10-15 Zernike polynomials. 2. Measure distance from tracker to segment to 0.6 mm. <ul style="list-style-type: none"> • equivalent to 1 μm rms defocus 3. Measure physical references at edge of segment to 1 mm. <ul style="list-style-type: none"> • limits focus and astigmatism to ~1 μm rms
Goals	
<ol style="list-style-type: none"> 1. Verify that focus and astigmatism are small enough to be corrected within ~half of 30 N rms force budget for active correction. 2. Determine radius of curvature to 0.5 mm. 3. Determine off-axis distance to 2 mm and clocking angle to 50 arcseconds. 	<ol style="list-style-type: none"> 1. Measure astigmatism accurate to 1 μm rms surface <ul style="list-style-type: none"> • correctable with 12 N rms force 2. Measure defocus accurate to 0.5 μm rms. <ul style="list-style-type: none"> • equivalent to 0.3 mm radius error • correctable with 17 N rms force 3. Measure distance from tracker to segment to 0.3 mm. 4. Measure physical references at edge of segment accurate to 0.5 mm. <ul style="list-style-type: none"> • equivalent to 25 arcseconds clocking
Ambitious goals	
<ol style="list-style-type: none"> 1. Verify that focus, astigmatism and coma are small enough to be corrected within 30 N rms force budget. 2. Determine radius of curvature to 0.3 mm. 3. Determine off-axis distance to 1 mm and clocking angle to 50 arcseconds. 	<ol style="list-style-type: none"> 1. Measure astigmatism accurate to 0.5 μm rms surface <ul style="list-style-type: none"> • corresponds to 1 mm change in off-axis distance • correctable with 6 N rms force 2. Measure coma accurate to 0.14 μm rms surface <ul style="list-style-type: none"> • correctable with 20 N rms force 3. Measure defocus accurate to 0.3 μm rms. <ul style="list-style-type: none"> • equivalent to 0.2 mm radius error • corresponds to 0.4 mm change in off-axis distance • correctable with 10 N rms force 4. Measure distance from tracker to segment to 0.2 mm. 5. Measure physical references at edge of segment accurate to 0.5 mm. <ul style="list-style-type: none"> • Equivalent to 25 arcseconds clocking, leaving room for astigmatism that looks like clocking.

2. LASER TRACKER PLUS SYSTEM DESCRIPTION

The Laser Tracker Plus system combines three measurement subsystems and a fourth positioning system to accurately measure the surface of the mirror during fabrication. The three measurement subsystems are a commercial laser tracker system, along with four distance measuring interferometers (DMI) and four position sensing detectors (PSD), which together form the external reference system that compensates for rigid-body motion and large-scale variations in refractive index. The fourth system is the SMR Positioning system, which moves the sphere-mounted retroreflector (SMR) between measurement locations across the surface of the mirror under test. A conceptual drawing of the Laser Tracker Plus system is shown in Figure 2.

2.1 Laser Tracker

A laser tracker is a commercial device that measures the position of a retroreflector in 3 dimensions by using a distance-measuring interferometer and two angular encoders. In its differential interferometer mode, it is sensitive to sub-micron displacements in the radial direction, and the encoder accuracy is on the order of 1 arcsecond. A laser tracker measures almost equally well for any surface geometry, making it a good choice for profiling the GMT surface. It is capable of measuring a mirror surface to sub-micron accuracy if the tracker is optimally located and if rigid-body motion of the mirror and tracker can be controlled during the course of the measurement, typically several minutes to an

hour. We have demonstrated this sort of accuracy in measurements of a 1.7 m off-axis mirror.⁹ To take advantage of the optimum orientation that maximizes the laser tracker's accuracy, the tracker should be mounted at the center of curvature (CoC) of the optic it is testing, thus minimizing the effect of angular errors on the surface measurement. For the case of GMT, this point is not accessible because its long RoC places the CoC beyond the roof of the lab, so the laser tracker is located as high above the GMT mirror segment as possible. The geometry for this system is shown in Figure 3.

The angle α describes the deviation of the line of sight from the surface normal, while $\delta\theta$ is the angular error in the laser tracker's measurement of the pointing angle θ . The resulting surface error due to the pointing error is

$$\delta s = r \sin \alpha \delta \theta,$$

where r is the radial distance measured by the laser tracker. For a spherical mirror, α can be calculated from

$$\sin \alpha = \frac{R-h}{R} \sin \theta = \frac{R-h}{R} \frac{x}{r},$$

where R is the RoC of the mirror, h is the height of the laser tracker above the mirror, and x is the lateral displacement of the SMR from the mirror center.

Using this, the sensitivity of the surface measurements to angular error in the line of sight of the tracker is

$$\frac{ds}{d\theta} = \frac{R-h}{R} r \sin \theta = \frac{R-h}{R} x.$$

The geometric parameters for a Laser Tracker Plus measurement of GMT are listed in Table 2. With $h = 22$ m (the tracker height above the mirror) and $R = 38$ m (the RoC), the sensitivity to angle is $1.7 \mu\text{m}/\mu\text{rad}$ at the outer edge of the mirror, while the average sensitivity to angle is $1.2 \mu\text{m}/\mu\text{rad}$ (the sensitivity at the 70% zone).

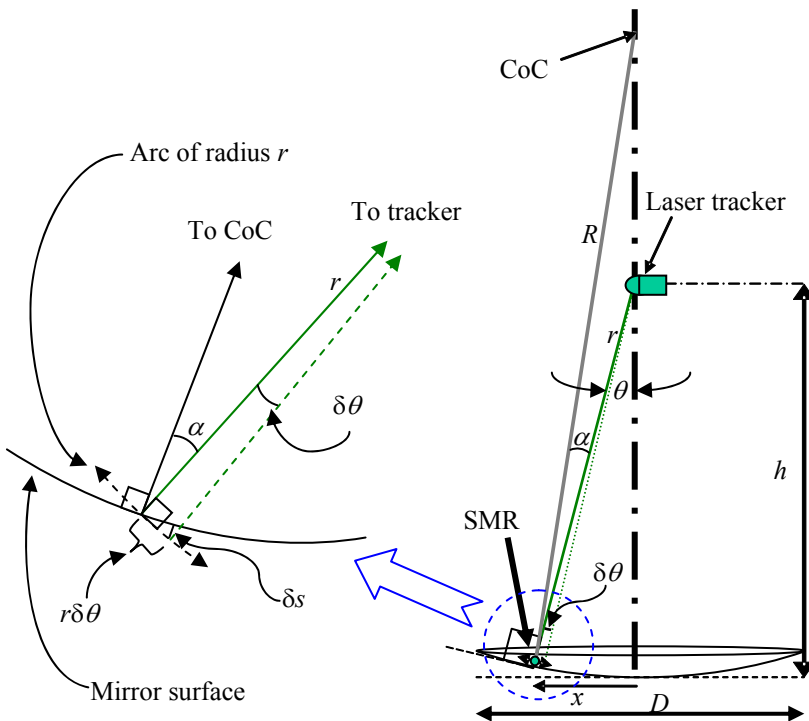


Figure 3: Geometry of the Laser Tracker Plus test setup for measuring GMT mirror segments. The closer the laser tracker is placed to the center of curvature (as $h \rightarrow R$), the closer the measurements are made to normal incidence ($\alpha \rightarrow 0$) and the less sensitive the measurements are to surface errors δs due to errors in the angles $\delta \theta$.

Table 2: Geometric parameters for a Laser Tracker Plus measurement of GMT.

Geometric Parameters	For GMT
Height of tracker above mirror (h)	22.3 m
ROC of mirror (R)	38 m
Diameter of mirror (D)	8.4 m
Maximum tracker scan angle (θ_{max})	10.7°
Tracker scan angle at 70% zone (θ_{ave})	7.5°
Maximum deviation of line of sight from surface normal (α_{max})	4.4°
Average deviation of line of sight from surface normal at 70% zone (α_{ave})	3.1°
Maximum sensitivity to angle ($ds/d\theta$)	1.7 $\mu\text{m}/\mu\text{rad}$
Average sensitivity to angle ($ds/d\theta$)	1.2 $\mu\text{m}/\mu\text{rad}$

2.2 External reference system

The external reference system is a system of stability references added to enhance the performance of a stand-alone laser tracker by compensating for rigid-body motion and large-scale variations in refractive index, as illustrated in Figure 4. The system includes four stand-alone DMIs, mounted on the same platform with the laser tracker, which monitor fixed retroreflectors at the edge of the mirror. They monitor the changes in the radial path length due to relative motion along the line of sight and changes in optical path length due to index variations. Some of the light from each of the DMIs is deflected to a PSD to monitor the lateral fluctuations of the reference laser beam perpendicular to the line of sight, including the effect of tilt of the laser tracker platform, and lateral motion of the beams due to relative motion of the mirror and laser tracker or index variations. This information is used to correct the laser tracker measurements of points on the mirror surface. The measurements of the reference arms are made simultaneously with the laser tracker measurements.

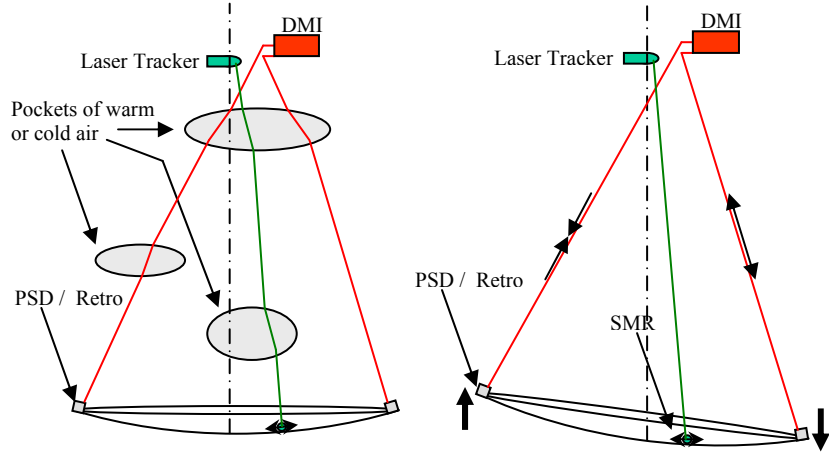


Figure 4: The external reference system is used to compensate for refractive index variations as shown in the figure on the left, and for relative motion between the test instruments and the mirror surface as shown in the figure on the right.

2.3 SMR positioning system

A measurement with the Laser Tracker Plus system consists of ~250 samples with 0.5 m spacing uniformly distributed over the surface. The system includes a mechanism that moves the SMR over the surface of the mirror safely under computer control. This allows mirrors up to 8.4 m diameter to be measured without people being on the mirror or its support platform. It minimizes changing loads that would cause rigid-body motion.

The 1.5 inch SMR is carried by an air puck that has three small flexible rubber air bearings that can glide across a polished surface without scratching. The SMR rests directly on the glass while tracker data are recorded. Air pressure is applied to lift the puck and SMR ~1 mm above the surface while the air bearings remain nearly in contact with the glass. The puck slides to the next position with minimal force, and slowly lowers the SMR to the surface as the air bleeds out. The puck is attached to four strings that control its position, as shown in Figure 5. The strings are controlled by motorized winches, two with position control and two holding constant tension. The winches and associated pulleys are mounted on steel beams about 3 m above floor level (slightly above the mirror surface) where they can be left permanently without interfering with traffic in the lab. Limit switches constrain the range of string positions so they cannot pull the SMR off the mirror or contact the four retroreflector/PSD assemblies at the edge of the mirror.

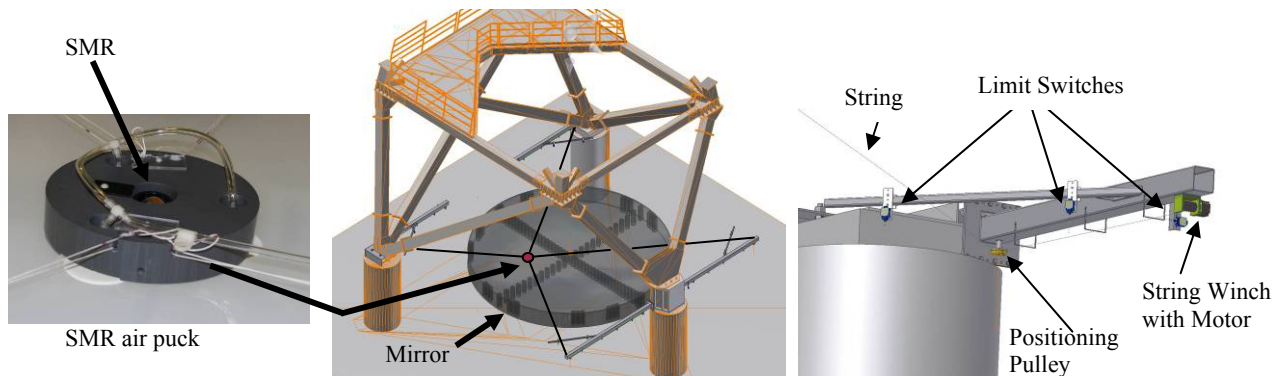


Figure 5: Diagram of the SMR positioning system at the base of the test tower. The gray disk represents the mirror under test, while the small circle at the intersection of the four strings is the location of the SMR puck. A close-up of one of the string control mechanism is shown on the right.

The SMR follows a pattern programmed into the control computer, pausing at each sample point long enough for the laser tracker and external reference system to make measurements before moving on to the next point. We aim to control the position to an accuracy of a few cm. The precise sample locations do not matter because the position is measured by the laser tracker.

3. CORRELATION RESULTS

A study was conducted using the Laser Tracker Plus system to compare the fluctuations measured by the stability references and the laser tracker, when the references and the SMR are mounted on the floor of the Steward Observatory Mirror Laboratory (SOML) test tower. The references were initially positioned on blocks on the floor so that they were nominally along the same lines of sight that they would be on if they were positioned around the edges of an 8.4 m mirror. A nest with a laser tracker SMR was placed atop the same block that the north surface reference was mounted on. Data were measured for an extended period of time with a 1 s measurement interval, which was decided to be a reasonable time interval for each measurement point and allows the individual measurement points to be averaged to evaluate the effect of integration time.

3.1 Radial correlation

The results of the radial correlation study show that over 5 minute time periods, the fluctuations measured by the laser tracker are about $0.07 \mu\text{m}$ rms, while the fluctuations measured by the DMIs for the same time was $0.2 \mu\text{m}$ rms, indicating that the DMIs are affected by environmental or instrumental noise more than the laser tracker. This means that if everything was stable during a measurement, then we would not want to apply the DMI correction, for that would just couple noise into the laser tracker measurements. However, during a typical GMT surface measurement, a significant amount of rigid-body motion does occur, as can be seen in Figure 6. Figure 7 shows data measured during the correlation study that shows the radial fluctuations measured by the laser tracker and DMIs are well correlated over longer time periods where there is an appreciable amount of motion, probably thermal expansion of the test tower. Because the systematics removed are large compared to the DMI noise added, making the correction improves the system accuracy.

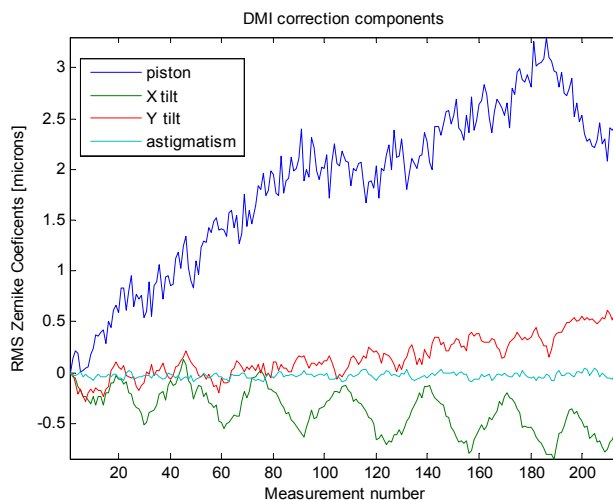


Figure 6: Plots showing the amount of the piston, tip, tilt, and astigmatism measured by the distance measuring interferometer reference system during a typical GMT measurement set. The negligible amount of astigmatism shows that almost all the motion can be described as rigid-body motion.

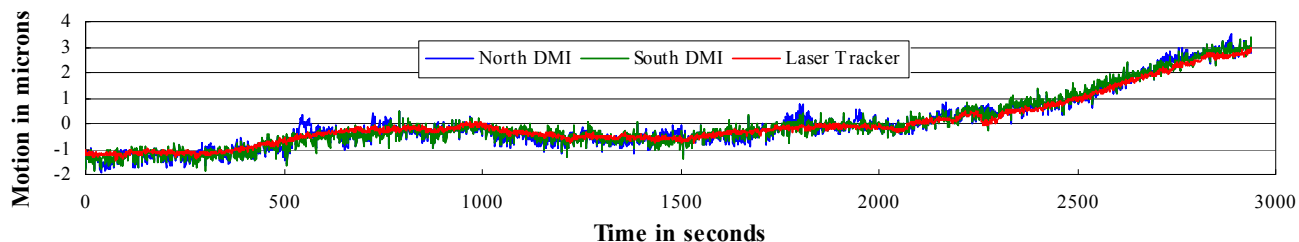


Figure 7: Comparison of radial fluctuations measured by the laser tracker and the north and south DMI references during 1 hour.

To apply the DMI correction, we fit the rigid-body motion to the four radial displacements of the reference arms, using the redundant information to check for inconsistencies in the reference data. The correction to the tracker measurement is obtained by taking the best-fit rigid-body displacement and evaluating it at the location of the SMR. Large-scale refractive index variations may look much like rigid-body motion and they can be corrected with the same recipe. If the variations are on such a small scale that there is little correlation between the effects at the SMR and the nearest reference arm, there is no point in applying a correction, and the way to improve the measurement is to average over a longer time.

From this portion of the study, the values for laser tracker radial noise of $<0.1 \mu\text{m}$ rms, DMI noise of $0.2 \mu\text{m}$ rms are added to Table 3. Also from Figure 6, plot labeled astigmatism shows that the non-planer motion measured by the DMIs is $<0.1 \mu\text{m}$ rms, which is listed as non-linear spatial variations in Table 3.

3.2 Angular correlation

The results of the angular correlation study show little or no correlation between the laser tracker and the PSD references. Over 5 minute time periods, the fluctuations measured by the laser tracker are about $0.4 \mu\text{rad}$ rms, while the fluctuations measured by the PSDs are $\sim 1.0 \mu\text{rad}$ rms, indicating that the PSDs are affected by environmental or instrumental noise more than the laser tracker. Figure 8 shows the angular fluctuations measured for the laser tracker during the same hour long data set that generated the radial plot in Figure 7, demonstrating that the laser tracker's angular fluctuations are only $0.5 \mu\text{rad}$ over the ~ 1 hour long time period required to make the GMT surface measurements. During a typical Laser Tracker Plus surface measurement, only about $0.3 \mu\text{rad}$ of systematic lateral motion of the mirror with respect to the laser tracker was observed, which is significantly less than the fluctuations in PSD measurements. Therefore, applying the PSD correction to the laser tracker surface measurements would couple more noise into the measurements than systematics removed, so we do not perform a PSD correction to the surface measurements. From this portion of the study, the values for laser tracker angular fluctuations of $0.5 \mu\text{rad}$ rms and uncompensated angular motion of $0.3 \mu\text{rad}$ rms are added to Table 3.

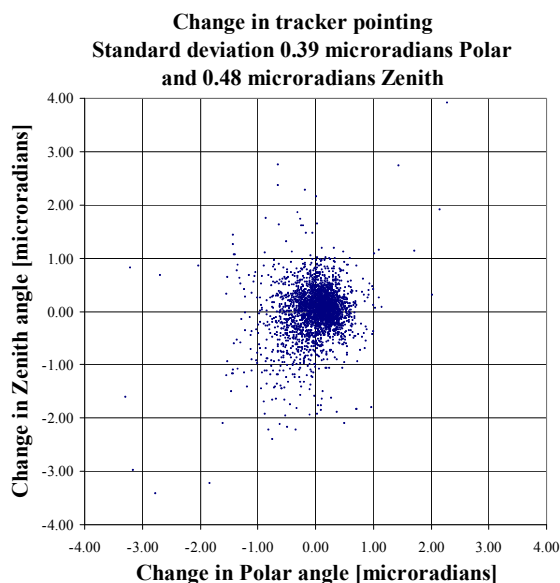


Figure 8: Typical measurement of angular fluctuations experienced by laser tracker over an hour.

4. CUSTOM LASER TRACKER CALIBRATION

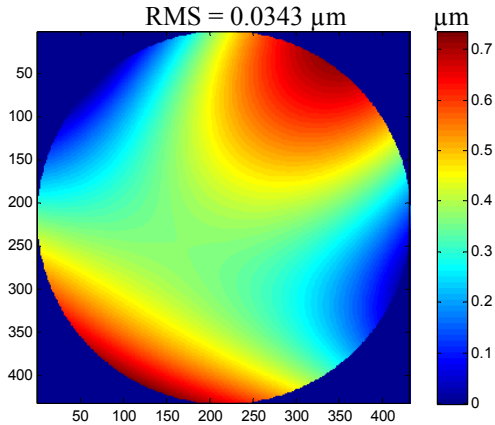
To improve the accuracy of the commercial laser tracker, a set of custom calibrations was devised to measure repeatable intrinsic errors in the laser tracker. There are both radial and angular calibrations to determine the repeatable errors in the laser tracker's measurement of radius as a function of angle, and angle as a function of angle.

4.1 Radial calibration

To calibrate the laser tracker's measurement of radial displacement, a small concave reference sphere was measured from its center of curvature. Because the radial distance was constant for all angles, the measurement was insensitive to angular errors, allowing a determination of the repeatable portion of the radial error. A 150 mm diameter $f/1.6$ spherical mirror was selected, covering a larger solid angle than the $f/2.6$ cone that an 8.4 m mirror subtends from the tracker.

Thirty separate measurements of the test mirror were made. Zernike polynomials were fit to each measurement, and the mean and standard deviation were calculated for each coefficient, which were used to generate the table and plot in Figure 9. The results of the radial calibration indicate that the radial errors in the laser tracker are negligible. The ambitious goal specified in Table 1 for the measurement accuracy of astigmatism is $0.5 \mu\text{m}$ rms surface, for coma is $0.14 \mu\text{m}$, and defocus is $0.3 \mu\text{m}$. Each one of these radial aberration errors was measured to be less than 1/10 of the goal values, therefore it was determined that no correction for radial errors was required. The standard deviation is larger than the mean for most of the coefficients in the calibration, indicating those values are mostly driven by measurement noise. Because the systematics are small compared to the uncertainty in the measurements, the correction should not be made, for this will couple more noise into the measurements than systematics removed, thus reducing the system accuracy. For this reason, the value of $\sim 0.05 \mu\text{m}$ of uncorrected systematic radial errors is included in Table 3 because no correction was applied.

Average of all 30 radial calibration data sets



Aberrations [$\mu\text{m rms}$]	Mean	St. Dev.
RMS of 3 rd degree fit	0.034	0.014
Astigmatism 0°	-0.031	0.013
Power	-0.012	0.011
Astigmatism 45°	0.000	0.012
Trefoil 0°	-0.004	0.011
Coma 0°	0.011	0.021
Coma 90°	0.008	0.018
Trefoil 30°	0.004	0.013

Figure 9: Average surface plot of the Zernike polynomial fit to the residual surface errors from all 30 radial calibration sphere measurements. The mean and standard deviation of all thirty data sets is provided in the table. Standard deviation is larger for most aberrations than the mean, so value of mean is mostly driven by noise.

4.2 Angular calibration

The 3D accuracy of a laser tracker measurement is limited by the angular component of the measurement. The purpose of the angular calibration is to improve the angular accuracy by performing a custom calibration of one laser tracker with the use of a second laser tracker. The laser tracker in the tower is calibrated by a second laser tracker mounted on the floor, as shown in Figure 10. The tracker in the tower measures horizontal displacement of an SMR with its angular encoders, while the floor-mounted tracker measures the same displacement much more accurately with its DMI. The SMR has a narrow angle of acceptance, so a fixture was designed to hold three 1.5 inch SMRs in direct contact along a straight line. The two outer balls were aimed upward toward the tracker to be calibrated, while the center ball was aimed horizontally toward the tracker on the floor. The location of the center ball is halfway between the two outer balls. The purpose of this is to eliminate sensitivity to offset errors from rotation of the fixture. The difference in the position of the fixture measured by the two laser trackers is used to determine the angular error in the upper tracker.

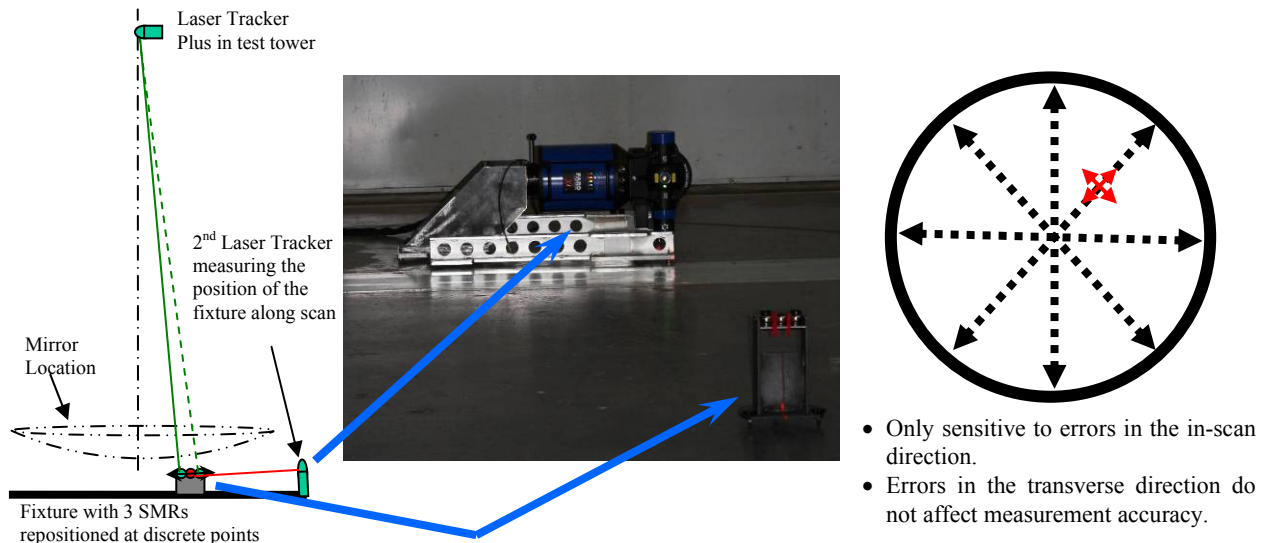


Figure 10: The diagram on the left shows the layout for the angular calibration. The laser tracker at floor measures the fixture location with small angular error compared to the tower tracker. The diagram on the right shows the pattern of multiple scans made to determine the discrepancy between the two trackers, which is used to determine a calibration correction for the angular errors.

Four scan lines angles were measured, two of them aligned to the rotation axes of the laser tracker in the tower, while the other two are the 45° lines in between. All four scans cross at the point directly beneath the laser tracker in the tower, where the error is defined to be zero. A 0.5 m measurement spacing was selected along each scan for a total of 21 measurements per scan over a 10 m scan diameter, which is approximately the diameter of the circle subtended by the GMT mirror when projected to the floor. For each scan, the floor laser tracker was set up so its line of sight is aligned to one of these scan lines. At each measurement position, the laser tracker at floor level measured the location of the center ball in interferometric mode (IFM), which uses a precision DMI to measure the radial displacements. At the same time, the tower tracker measured the location of the outer two outer balls in absolute distance mode, which determines the radial distance by modulating the laser beam. The two outer ball measurements are then averaged together. The assumption is that the laser tracker at the floor measuring in IFM with its DMI has much better accuracy than the tracker in the tower, so any discrepancy between the two sets of measurements is an angular error in the tower tracker.

The difference between the two trackers' measured in-scan distance change is the angular error in the laser tracker along each of the four scan angles. The four scans are fit by polynomials, for instance Zhao's \bar{s} polynomials, to interpolate the angular error across the mirror.¹⁰ These polynomials are reduced from regular standard Zernike polynomials by one power of r , and when multiplied by the mirror sensitivity, which is proportional to r , the result is a set of basis functions for the surface error that have the same form as standard Zernike polynomials, with some differences in the normalization. From the polynomials fit, the angular error is computed at each surface measurement location and the angular values measured by the laser tracker are modified to account for the error. Plots of the calculated angular correction based on the averaged results of three angular calibration measurements are shown in Figure 11.

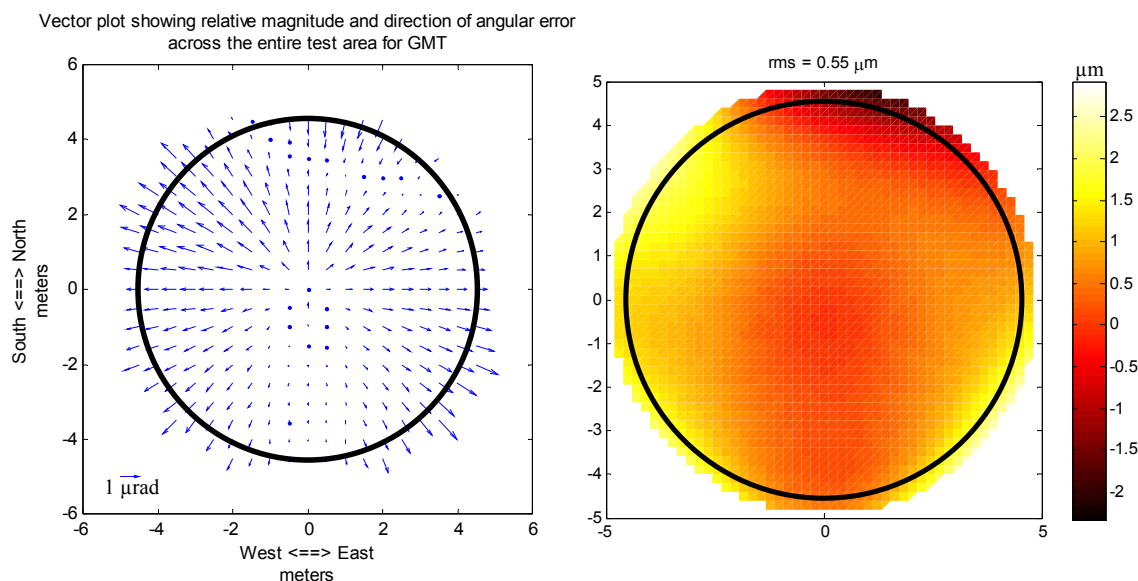


Figure 11: The left hand plot shows the laser tracker angular error in the radial direction based on the average of the three sets of scans. The right hand plot shows the expected surface error in the laser tracker measurements due to these angular errors. The black circle represents the area of the test subtended by the GMT mirror. The surface error over the GMT mirror that can be corrected by applying this angular calibration is $0.55 \mu\text{m}$ rms.

The results of the angular calibration indicate that there is $\sim 0.62 \mu\text{rad}$ rms of angular errors before applying the correction, which is consistent with the combination of $0.35 \mu\text{rad}$ rms of random angular errors, the in-scan component of tracker angular fluctuations discussed in Section 3, and $\sim 0.50 \mu\text{rad}$ rms of systematic angular errors. The predicted residual error after applying the correction is reduced to $\sim 0.52 \mu\text{rad}$ rms, which indicates that the systematic angular errors have been reduced to $\sim 0.38 \mu\text{rad}$ rms, so this value has been included in Table 3. By reducing these angular systematic errors further, the system accuracy could be further improved. The Zhao's \bar{s} polynomials were used for fitting the angular calibration data because we expected that the laser tracker angular errors would look like low-order distortions, which the \bar{s} polynomials are typically used for fitting. The reality is that errors that were measured are not well fit by this particular set of functions, and further work could be done to determine another set of functions that give better results by reduce the systematic errors further.

5. SYSTEM ACCURACY

A straightforward measurement of an optical surface with a commercial laser tracker at a distance of 22 m is expected to give an accuracy of 5-10 μm rms per sample point. Due to the enhancements of the Laser Tracker Plus system, we expect that the system accuracy will be significantly better than this. The system accuracy is improved by using separate systems to measure the intrinsic and environmental errors and provide corrections to improve the measurement accuracy, but these other systems also have errors that limit the ultimate accuracy. The corrections are imperfect, so only a portion of the real systematic errors are actually corrected, while some portions remain uncorrected. Additionally, some portion of the correction is wrong, so non-repeatable errors or random fluctuations get coupled into the correction; these errors will actually reduce the system accuracy. If the systematic errors are larger than the uncertainty in the correction, then the system accuracy is improved by making the correction. If the systematics are small compared to the uncertainty in the measurements, then the correction should not be made.

Table 3 lists the Laser Tracker Plus system accuracy. The values are based on errors determined during the correlation study and the calibration measurements. Another potential source of error is the SMR geometry (displacement between the cube vertex and the ball center), but its impact on the surface measurement is $< 0.01 \mu\text{m}$.

Table 3: Laser Tracker Plus system accuracy in rms surface.

Laser Tracker Plus System Measurement Accuracy for GMT					
Category	Source	Type	Direct surface microns	Angle microradians	Net surface microns
Tracker Calibration					
Distance vs angle:	Uncorrected systematics	systematic	0.05		0.05
Angle vs angle:	Uncorrected systematics	systematic		0.38	0.46
Tracker Fluctuations					
	Distance (noise only)	random	0.10		0.10
	Angle (total fluctuation)	random		0.50	0.60
Compensation					
Distance:	DMI noise	random	0.20		0.20
	Non-linear spatial variation	random	0.10		0.10
Angle:	Uncompensated motion	random		0.30	0.36
Net Error			0.25	0.70	0.87

The radial errors directly contribute to errors in the surface measurements, while the angular errors couple to surface errors through the sensitivity relationship described in Section 2.1. For GMT, the average sensitivity is $1.2 \mu\text{m}/\mu\text{rad}$, which is multiplied with the angular errors in Table 3 to determine the resulting net surface errors. These errors are then root-sum-squared to determine the expected net error for the entire system. The result is that the GMT surface measurement is expected to be accurate to better than $0.87 \mu\text{m}$ rms, which compares well to the goal of $< 1 \mu\text{m}$ rms listed in Table 1.

An estimate was performed to determine how the error sources listed in Table 3 couple into the low-order Zernike polynomials that the Laser Tracker Plus system is expected to verify for the principal test. The error sources were each classified as either random or systematic, and their magnitude was multiplied by a scale factor to give the coupling of the error into each polynomial coefficient. The random errors contribute equally to all the polynomials by a scale factor of $1/\sqrt{N} \approx 0.06$, where N , the number of measurement points, is 256 for a typical surface measurement. Coupling factors for systematic errors must be estimated. The worst case for any aberration would be a coupling factor of 1.0, leaving no systematic error in any other aberration. Instead, the assumption was made that systematic errors will couple more strongly into the simpler and more systematic aberrations: 0.5 for power, 0.3 per component of astigmatism, and 0.2 per component of coma. Table 4 lists the expected error in the fit for these three critical Zernike polynomials as a result of the individual measurement errors.

The ADM error is a special case that only affects the focus term, so it was not listed in Table 3. It refers to the measurement of absolute distance between the tracker and the mirror surface. A scan consists of a single absolute measurement followed by ~ 250 differential samples. The ADM error causes an error in RoC, equivalent to focus in the surface ($0.0018 \mu\text{m}$ rms surface focus per micron of distance error). The laser tracker used has a listed ADM accuracy of

$\pm (9.8 \mu\text{m} + 0.4 \mu\text{m}/\text{m})$, which at a distance of 22.3 m works out to an initial distance uncertainty of $\pm 18.7 \mu\text{m}$, which agrees with the values typically observed. This error is very small and contributes $< 0.03 \mu\text{m}$ rms of error in the focus coefficient.

Table 4: Expected errors in the fit of low-order Zernike polynomials in microns rms surface to a GMT surface measurement due to the errors listed in Table 3 for individual Laser Tracker Plus measurements. Values for astigmatism and coma are for the two components combined ($\sqrt{2}$ times the error in each component). These values meet the system design specifications listed in Table 1.

Error Contributions to Zernike Polynomials for GMT					
Category	Source	Type	Focus	Astigmatism	Coma
			microns	microns	microns
Tracker Calibration					
Distance vs angle:	Uncorrected systematics	systematic	0.03	0.02	0.01
Angle vs angle:	Uncorrected systematics	systematic	0.23	0.19	0.13
Tracker Fluctuations					
	Distance (noise only)	random	0.01	0.01	0.01
	Angle (total fluctuation)	random	0.04	0.05	0.05
Compensation					
Distance:	DMI noise	random	0.01	0.02	0.02
	Non-linear spatial variation	random	0.01	0.01	0.01
Angle:	Uncompensated motion	random	0.02	0.03	0.03
ADM Error					
	Initial distance measurement	systematic	0.03		
RMS Surface Error			0.24	0.21	0.15

6. COMPARISON OF LASER TRACKER PLUS & OPTICAL MEASUREMENTS

Measurements with the Laser Tracker Plus system are in reasonably good agreement with the GMT optical test.¹¹ Figure 12 shows the most recent measurements of each, with and without focus and astigmatism. The Laser

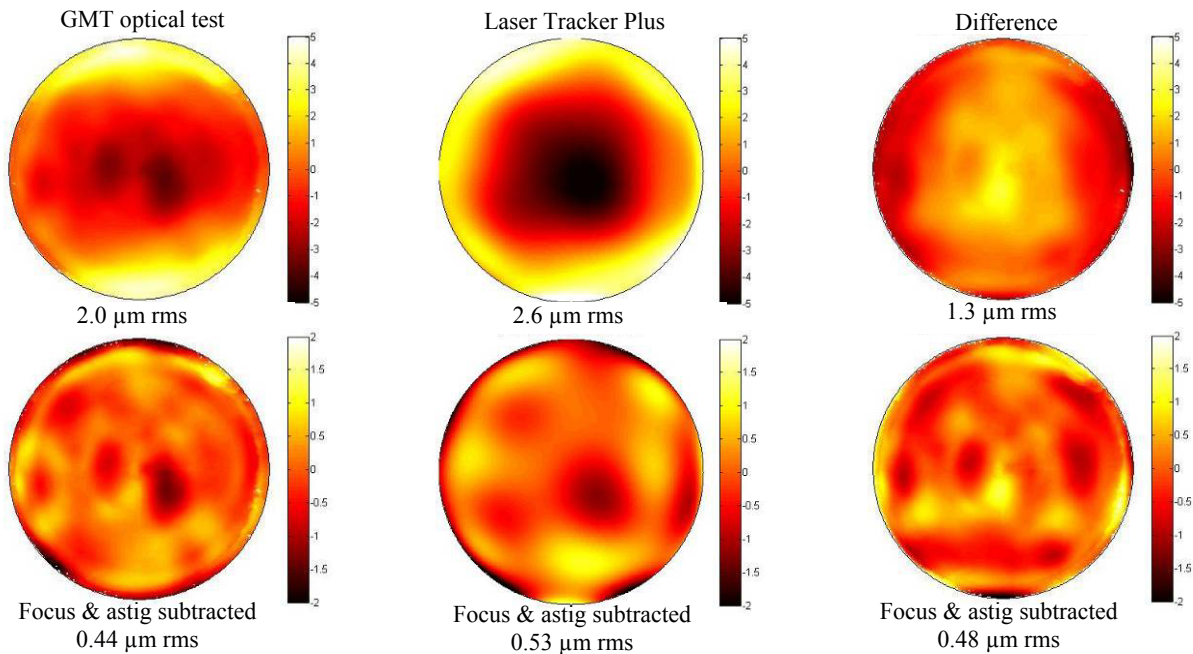


Figure 12: Comparison of measurements with the GMT optical test (left) and the Laser Tracker Plus system (center). The two measurements and their difference are shown with no adjustments (top) and with focus and astigmatism subtracted (bottom). Color bars and values listed are microns of surface error.

Tracker Plus map is an 8th degree polynomial fit to the 256 measured points (0.5 m sampling). The differences in focus (1.0 μm rms surface) and astigmatism (0.7 μm rms) are 3-4 times the target accuracy for the Laser Tracker Plus, but we expect that small misalignments in the early implementation of the GMT optical test, and temperature gradients in the segment, are contributing significant errors in these aberrations. These additional sources of error will be reduced as the alignment of the optical test is refined⁶ and the segment temperature is controlled more precisely in the final stage of fabrication. With focus and astigmatism subtracted, much of the difference is small-scale structure that the Laser Tracker Plus does not resolve.

7. SUMMARY

The Laser Tracker Plus system is a mature system that can measure large, asymmetric optical surfaces to an accuracy of better than 1 μm rms surface in all aberrations including focus. It works on ground or polished surfaces, was used to guide the figuring of the GMT segment to the point of hand-off to the visible interferometric test, and serves to validate the visible test in the low-order aberrations.

ACKNOWLEDGMENTS

This material is based in part on work supported by AURA through the National Science Foundation under Scientific Program Order No. 10 as issued for support of the Giant Segmented Mirror Telescope for the United States Astronomical Community, in accordance with Proposal No. AST-0443999 submitted by AURA.

REFERENCES

- [1] J. H. Burge, L. B. Kot, H. M. Martin, C. Zhao, and T. Zobrist, "Alternative surface measurements for GMT primary mirror segments", in *Optomechanical Technologies for Astronomy*, Proc. SPIE **6273**:62732T (2006).
- [2] T. Zobrist, J. H. Burge, W. B. Davison, and H. M. Martin, "Measurements of large optical surfaces with a laser tracker", in *Advanced Optical and Mechanical Technologies in Telescopes and Instrumentation*, Proc. SPIE **7018**:70183U (2008).
- [3] H. M. Martin, J. H. Burge, B. Cuerden, W. B. Davison, J. S. Kingsley, W. C. Kittrell, R. D. Lutz, S. M. Miller, C. Zhao, and T. Zobrist, "Progress in manufacturing the first 8.4 m off-axis segment for the Giant Magellan Telescope", in *Advanced Optical and Mechanical Technologies in Telescopes and Instrumentation*, Proc. SPIE **7018**:70180C (2008).
- [4] M. Johns, "Progress on GMT", in *Advanced Optical and Mechanical Technologies in Telescopes and Instrumentation*, Proc. SPIE **7018**:70121B (2008).
- [5] J. H. Burge, W. Davison, C. Zhao, and H. M. Martin, "Development of surface metrology for the Giant Magellan Telescope primary mirror", in *Advanced Optical and Mechanical Technologies in Telescopes and Instrumentation*, Proc. SPIE **7018**:701814 (2008).
- [6] S. C. West, J. H. Burge, B. Cuerden, W. B. Davison, J. Hagen, H. M. Martin, M. T. Tuell and C. Zhao, "Alignment and use of the optical test for the 8.4m off-axis primary mirrors of the Giant Magellan Telescope", in *Modern Technologies in Space and Ground Based Telescopes and Instrumentation*, Proc. SPIE **7739**:773921 (2010).
- [7] T. Zobrist, J. H. Burge, and H. M. Martin, "Laser tracker surface measurements of the 8.4 m GMT primary mirror segment", in *Optical Manufacturing and Testing VIII*, Proc. SPIE **7426**:742613 (2009).
- [8] J. H. Burge, L. B. Kot, H. M. Martin, C. Zhao, and R. Zehnder, "Design and analysis for interferometric testing of the GMT primary mirror segments", in *Optomechanical Technologies for Astronomy*, Proc. SPIE **6273**:62730M (2006).
- [9] H. M. Martin, J. H. Burge, S. D. Miller, B. K. Smith, R. Zehnder, and C. Zhao, "Manufacture of a 1.7-m prototype of the GMT primary mirror segments", in *Optomechanical Technologies for Astronomy*, Proc. SPIE **6273**:62730G (2006).
- [10] C. Zhao and J. H. Burge, "Orthonormal vector polynomials in a unit circle, Part I: basis set derived from gradients of Zernike polynomials", *Optics Express*, **15**:18014 (2007).
- [11] H. M. Martin, R. G. Allen, J. H. Burge, D. W. Kim, J. S. Kingsley, M. Tuell, S. C. West, C. Zhao, and T. Zobrist, "Fabrication and testing of the first 8.4 m off-axis segment for the Giant Magellan Telescope", in *Modern Technologies in Space and Ground Based Telescopes and Instrumentation*, Proc. SPIE **7739**:773909 (2010).